A Miniature MRI-Compatible Fiber-optic Force Sensor Utilizing Fabry-Perot Interferometer

Hao Su[*§1], Michael Zervas[§2], Cosme Furlong[2] and Gregory S. Fischer[1]

[1]Automation and Interventional Medicine (AIM) Robotics Laboratory

Department of Mechanical Engineering, Worcester Polytechnic Institute, Worcester, MA, USA

[2]Center for Holographic Studies and Laser micro-mechaTronics

Department of Mechanical Engineering, Worcester Polytechnic Institute, Worcester, MA, USA

*Corresponding author: haosu@wpi.edu, (508)-831-5191. §Shared first authorship.

ABSTRACT

Magnetic resonance imaging provides superior imaging capability because of unmatched soft tissue contrast and inherent three-dimensional visualization. Force sensing in robot-assisted systems is crucial for providing tactile feedback and measuring tissue interaction forces in needle-based percutaneous procedures in MRI. To address the issues imposed by electromagnetic compatibility in the high-field MRI and mechanical constraints due to the confined close-bore space, this paper proposes a miniaturized fiber optic force sensor utilizing Fabry-Perot interferometry. An opto-electromechanical system is designed to experimentally validate the optical model of the sensor and evaluate its sensing capability. Calibration was performed under static and dynamics loading conditions. The experimental results indicate a gage sensitivity on the order of 40 (mV/με) of the sensor and a sensing range of 10 Newton. This sensor achieves high-resolution needle insertion force sensing in a robust and compact configuration in MRI environment.

Keywords: Optical Force Sensor, Fabry-Perot Interferometer, MRI Compatibility, Needle Insertion

I. INTRODUCTION

Magnetic resonance imaging (MRI) is a multi functional imaging modality with unmatched soft tissue contrast that allows for accurate delineation of the pathologic and surrounding normal structures and inherent three-dimensional visualization that permits dynamic imaging plane control and surgical tool tracking. Comparing with ultrasound and computerized tomography, it has an unparalleled potential for guiding, monitoring and controlling therapy in real-time. D'Amico *et. al* [1] reports that the positive predictive value of transrectal ultrasound-guided needle biopsy is only 18% to diagnose prostate cancer, while MRI-guided prostate brachytherapy and biopsy procedure achieved 100% dose coverage within the prostate without exceeding the maximal allowable doses using a 0.5T open-MRI scanner. In general, MRI allows for interventional surgery in an efficient and high-accuracy manner.

Due to intrinsic MRI compatibility, there are significant research efforts on optical force sensing recently. It is immune to electromagnetic signal and resistant to harsh environment. The intensity modulated optical sensor, based on optical micrometry or reflected mirror [2-3], is convenient to design and manufacture. However, it is sensitive to environment change and usually bulky thus impractical for a large range of force sensing to be integrated with surgical tools (e.g. needles, electrodes and catheters). Fiber Bragg Grating (FBG) sensor [4], a wavelength modulated approach, provides an amiable solution with high sensing senility and miniaturization. FBG directly correlate the wavelength of light and the change in the desired strain. If the fiber is strained from applied loads then these gratings will change accordingly and allow a different wavelength to be reflected back from the fiber. Nevertheless, the costly optical source and spectral analysis equipment (usually more than $20K) present formidable application for medical instrumentation. Based on our previous efforts on MRI-compatible piezoelectric actuation and robot design [5-10], the aim of this paper is to design a miniaturized fiber optic force sensor that can be integrated with the robotic systems.

This paper investigates Fabry-Perot interference (FPI) fiber optic sensor for several advantages over other fiber optic sensors [11]. First, in contract to intensity modulated techniques, FPI is phase modulated and provides absolute force measurement, independent of light source power variations. Second, because it takes advantage of multimode fiber and minimizes adverse

effect of thermal and chemical changes. Besides, it can be miniaturized in meso-scale and integrated to surgical tools. In addition to biocompatibility, it is sterilization tolerant with ethylene oxide and autoclave. The operating temperature is −40oC to 250oC. The sensing strain ranges from ±1000 με to ±5000με with resolution1 0.01% of full scale.

To our knowledge, the work in this paper is the first investigation of FPI sensors in needle insertion force measurement with a focused application in MRI-guided prostate interventions. This paper is organized as follows: Section II describes the FPI sensing principle of Fabry-Perot interference sensor. Section III presents the design and mechanical modeling of FPI sensor. Opto-mechanical design to implement FPI is presented in Section IV. Sensor calibration and experimental validation is presented in Section V. In Section VI, we conclude with a discussion of FPI sensor and future work.

II. SENSING PRINCIPLE OF FABRY-PEROT INTERFEROMETER

In a Fabry-Perot strain sensor, light propagates through a cavity containing semi-reflective mirrors. Some light is transmitted and some is reflected. As shown in Fig. 1, the distance between the two fiber tips is generally on the order of nanometers and depends on the gauge length (the active sensing region, defined as the distance between fusion welds). L_{cavity} is the original cavity length. δ is the change in the cavity length from a given load. The returning light interferes resulting in black and white bands known as fringes caused by destructive and constructive interference. The intensity of these fringes varies due to a change in the optical path length related to a change in cavity length when uni-axial force is applied.

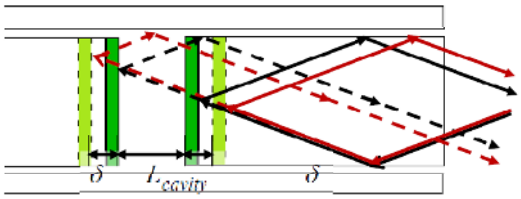

Fig. 1: Light Propagation through FPI Cavity

This phenomenon can be quantified through the summation of two waves [12]. By multiplying the complex conjugate and applying Euler's identity, we obtain the following equation of reflected intensity at a given power for planar wave fronts:

$$I = A_1^2 + A_2^2 + 2A_1^2A_2^2\cos(\phi_1 - \phi_2) \quad [1]$$

with A_1 and A_2 representing the amplitude coefficients of the reflected signals. The above equation can be changed to represent only intensities by substituting $A_i^2 = I_i(i = 1,2)$ and $\phi_1 - \phi_2 = \Delta\phi$ as

$$I = I_1 + I_2 + 2\sqrt{I_1I_2}\cos(\Delta\phi) \quad [2]$$

III. MECHANICAL MODELING OF FABRY-PEROT INTERFEROMETER SENSOR

An FPI fiber optic strain sensor (FISO Technologies, Canada) [13] was used to evaluate the systems resolution and potential integration into the robot. As shown in Fig. 2, the main component of the FPI is the sensing cavity, measuring 15.8 μm wide. A glass capillary covering the sensing region is fusion welded to the fiber in two locations and encapsulates the sensor. There is an air gap of approximately 100.5 μm wide. The total length of the FPI sensor, including the glass capillary, and bare fiber is approximately 20mm. Besides immune to electromagnetic and RF signal and substantially cheaper than FBG, the advantages of this sensor includes: 1) static/dynamic response capability, 2) high sensitivity and resolution, 3) no interference due to cable bending and 4) robust to a large range of temperature variation (-40º-250º) due to air gap insulation to the sensing region.

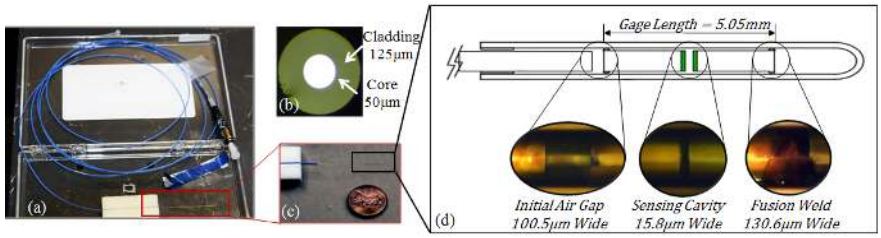

Fig. 2: Miniaturized Fabry-Perot Interferometer Strain Sensor (a) Commercially Available FISO Technologies FPI strain sensor (b) Fiber tip under microscope (c) Size perspective of sensor (d) Expanded view of components of FPI strain sensor

Finite element analysis software, ANSYS Workbench [14], was utilized to develop a three-dimensional model of FPI sensor. A CAD model was imported into ANSYS Workbench with the correct constraints, applied force, and material properties just as in the analytical model as seen in Fig. 3 (left). The ANSYS contained a great deal more elements and nodes than the analytical model with 8076 elements and 22,183 nodes. After the complex model was tested and the results were analyzed, comparisons between the analytical and computational calculations were made.

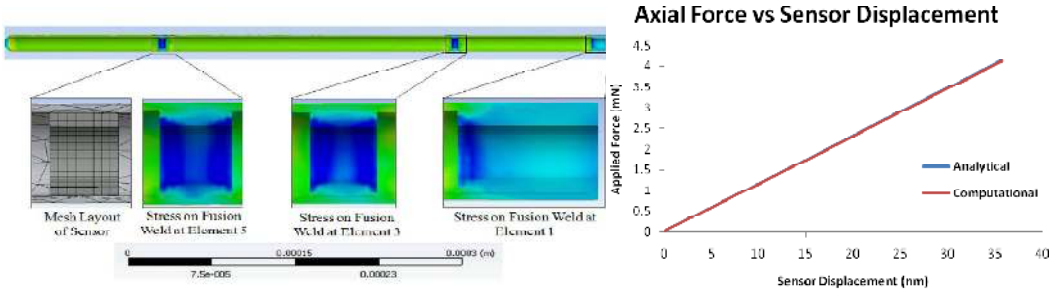

Fig. 3: (left) ANSYS Computational Model of FPI, and (right) Analytical and Computational Agreement of Linearity of FPI Sensor

As Fig.3 (right) depicts, there is a nearly perfect agreement between the analytical and computational calculations with less than 1% error between them. Since the FPI sensor's linearity was verified using two different finite element methods, we now had to set out on designing an opto-mechanical setup for use of our FPI sensor.

IV. OPTO-MECHANICAL DESIGN

The opto-mechanical setup begins with a pigtailed laser diode (PLD) which emits light in the 830nm band of the infrared line with a power of 1mW. This diode is controlled by a laser diode controller (LDC) which has a PID built in which helps stabilize the temperature and current of the diode when attached to laser cooler. The output of the pigtailed laser that exits the FC connector (FC) at the end of the sensor's fiber is connected to a Z-axis translator (ZT). This Z-axis translator helps focus the divergent light onto a 20× objective lens mounted to an X- Y-axis translator (20XYT). This collimated light is sent into a 50:50 beam splitter cube (BS) where fifty percent of the light is split towards the FPI and the other fifty percent is not used.

The light that is sent to the sensor is focused onto the 50μm core of the sensor's multimode fiber. This focusing is accomplished with the help of another 20× objective lens mounted to an X-Y-axis translator which focuses the light onto the fiber core which is able to adjust via a Z-axis translator which has the FPI fiber's ST connector (ST) attached to it. The light travels through the fiber and into the sensing cavity and then back reflects out the same optical axis it came in. This back reflected light passes through the 20X objective lens and is collimated into the beam splitter and once through the beam splitter the light is sent into the photodetector (PD). The photodetector's output is digitized by a 16-bit data acquisition system (DAQ) and a processing computer (PC) is used to calculate the strain values.

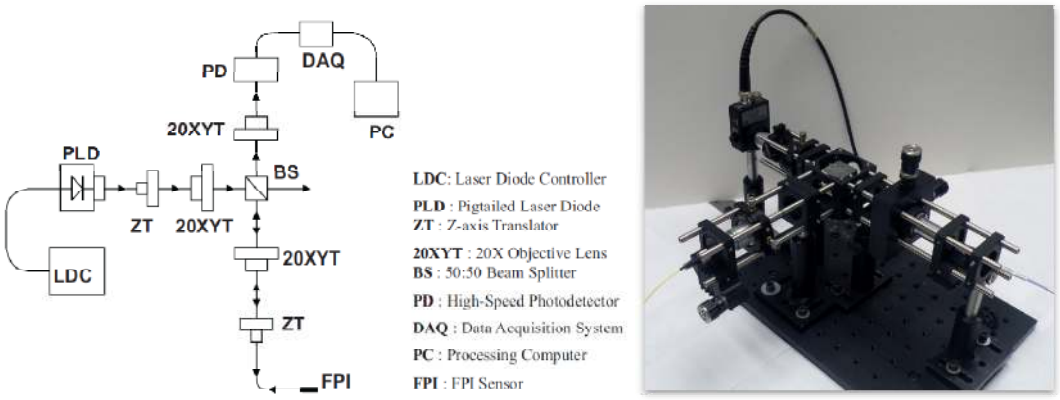

Fig. 4: (left) Schematic diagram of the opto-mechanical design to implement FPI sensor and (right) the bench top evaluation system of opto-mechanical design to implement FPI sensor.

V. FIBER OPTIC FORCE SENSOR CALIBRATION

Calibration was performed by attaching the FPI to a manufactured cantilever beam made of aluminum 6063-T5. Strain on the beam was calculated in terms of the applied force F:

$$\varepsilon_{xx} = \frac{12FLc}{bt^3E} \quad [3]$$

where L is the length of the beam, c is the distance from the center of the beam along the y-direction, b is the width of the base, t is the thickness, and E is Young's modulus.

In order to calibrate the FPI, the relationship between the intensity of light at the output and the strain was derived. A hanger system was employed at the end of the cantilever beam to statically apply the load in increments of the 5 grams. Each of the weights used were weighted on a calibrated scale. The opto-mechanical setup was used to measure the output light intensity from the FPI and was recorded using the LabView program [15].

Recall in equation 2, the change in phase $\Delta\phi$ of the intensity equation is equal to the wave number $\frac{2\pi}{\lambda}$, multiplied by the length of the sensing cavity region and the strain in the x-direction:

$$\Delta\phi = \frac{2\pi(\varepsilon_{xx}L_{cavity})}{\lambda} \quad [4]$$

This value for the change in phase was substituted into intensity equation and it is now possible to predict the output intensity of light as a function of the induced strain:

$$I = 2I_0[1 + \cos(\frac{2\pi(\varepsilon_{xx}L_{cavity})}{\lambda})] \quad [5]$$

The calibrated system can be seen in the voltage-strain graph shown in Fig. 5. The theoretically predicted relationship is superimposed in the figure. The output voltage follows a sinusoidal pattern that repeats over an increasing applied force. A LabView program is built to count cycles as the interference pattern repeats between a maximum and minimum voltage range, which allows users to accurately determine the applied force. The discrepancy between the measurement and theoretical model is due to the ambient light disturbance to the opto-mechanical prototype which is not shielded during experiment. An optical packaging system with compact structure and light shielding is under development. Depending on the required resolution, the FPI sensor can be calibrated to remain within a $\frac{\pi}{4}$ cycle for a maximum applied force of 10 Newton that directly correlates voltage to force and avoids counting cycle. A gage factor of 40mV/με was calculated and when using a 16 bit data acquisition system, the FPI sensor is able to measure a minimum strain value of approximately 6.4 nano strains.

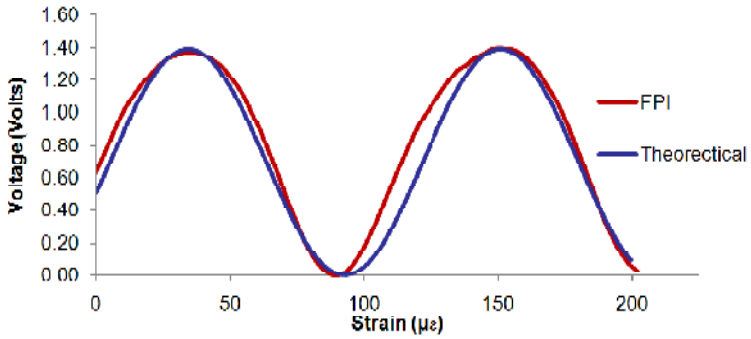

Fig. 5: Calibration results showing voltage versus strain of the FPI sensor overlaid with the theoretical model.

VI. CONCLUSION AND DISCUSSION

A fiber optic force sensor based on Fabry-Perot interferometry is modeled and calibrated. Comparisons between the fiber optic sensor and a typical foil strain gauge proved the FPI was superior in aspects including immunity to electromagnetic waves and resolution. Future testing should be done on this sensor to evaluate its performance and durability in MRI scanner room.

The next step of this work will focus on packaging the opto-mechanical system and attain robust and portable interface with the robot controller. The measured needle insertion force can be used to inferred tissue stiffness properties and increase the cancer detection rates.

VII. REFERENCES:

[1] D'Amico A. V., Cormack R. A. and Tempany C. M., "MRI-guided diagnosis and treatment of prostate cancer". New England Journal of Medicine, volume 344(10), pp. 776-7, 2001.

[2] Polygerinos P., Puangmali P., Schaeffter T., Razavi R., Seneviratne L., and Althoefer K., "Novel miniature MRI-compatible fiber-optic force sensor for cardiac catheterization procedures," in Robotics and Automation (ICRA), 2010 IEEE International Conference on, pp. 2598–2603, May 2010.

[3] Su H. and G. Fischer, "A 3-axis optical force/torque sensor for prostate needle placement in magnetic resonance imaging environments," 2nd Annual IEEE International Conference on Technologies for Practical Robot Applications, (Boston, MA, USA), pp. 5–9, IEEE, 2009.

[4] Park Y.-L., Elayaperumal S., Ryu S., Daniel B., Black R. J., Moslehi B., and Cutkosky M., "MRI-compatible Haptics: Strain sensing for real-time estimation of three dimensional needle deflection in MRI environments," in International Society for Magnetic Resonance in Medicine (ISMRM), 17th Scientific Meeting and Exhibition, (Honolulu, Hawaii), 2009.

[5] Su H. and Fischer G. S., "High-field MRI-Compatible needle placement robots for prostate interventions: pneumatic and piezoelectric approaches," in Advances in Robotics and Virtual Reality (T. Gulrez and A. Hassanien, eds.), Springer-Verlag, 2011.

[6] Huang H., Su H. and, Mills J., "Force Sensing and Control of Robot-Assisted Cell Injection", eds. T. Gulrez and A. Hassanien, Advances in Robotics and Virtual Reality, Springer-Verlag, 2011

[7] Wang Y., Cole G., Su H., Pilitsis J., and Fischer G., "MRI compatibility evaluation of a piezoelectric actuator system for a neural interventional robot," in Annual Conference of IEEE Engineering in Medicine and Biology Society, (Minneapolis, MN), pp. 6072–6075, 2009.

[8] Cole G., Harrington K., Su H., Camilo A., Pilitsis J., and Fischer G.S., "Closed-Loop Actuated Surgical System Utilizing Real-Time In-Situ MRI Guidance," in 12th International Symposium on Experimental Robotics - ISER 2010, (New Delhi and Agra, India), Dec 2010.

[9] Wang Y., Su H., Harrington K., and Fischer G. S., "Sliding mode Control of piezoelectric valve regulated pneumatic actuator for MRI-compatible robotic intervention," in ASME Dynamic Systems and Control Conference - DSCC 2010, (Cambridge, MA, USA), 2010.

[10] Su H., Camilo A., Cole G., Tempany C.M., Hata N. and Fischer G. S., " High-Field MRI Compatible Steerable Needle Driver Robot for Percutaneous Prostate Intervention", Proceedings of MMVR18 (Medicine Meets Virtual Reality), Newport Beach, California, USA, February, 2011

[11] Lemay J., White F., Zervas M., "Evaluation and Application of a High Resolution Fiber-Optic Strain Sensor", Major Qualifying Project, Dept. of Mechanical Engineering, Worcester Polytechnic Institute, April. 2010.
[12] Gangopadhyay T. K., "Prospects for fiber Bragg gratings and Fabry-Perot interferometers in fiber-optic vibration sensing," Sensors and Actuators A: Physical, vol. 113, no. 1, pp. 20 – 38, 2004.
[13] RocTest Limited, FISO Technologies, Inc., Sensoptic Fiber-Optic Strain Sensors - Fabry-Perot Strain Gage – FOS Series. Quebec, Canada: RocTest, 2000
[14] ANSYS, "ANSYS Academic Teaching Mechanical," Accessed 15 February 2010
[15] National Instruments. Retrieved April 12, 2010, from www.ni.com